



# Halogen Enrichment of Siberian Traps Magmas During Interaction With Evaporites

Svetlana Sibik<sup>1</sup>, Marie Edmonds<sup>1\*</sup>, Benoit Villemant<sup>2</sup>, Henrik H. Svensen<sup>3</sup>, Alexander G. Polozov<sup>4</sup> and Sverre Planke<sup>3,5</sup>

<sup>1</sup>Department of Earth Sciences, University of Cambridge, Cambridge, United Kingdom, <sup>2</sup>ISTEP, Sorbonne Université, Paris, France, <sup>3</sup>Centre for Earth Evolution and Dynamics (CEED), Dept. of Geosciences, University of Oslo, Oslo, Norway, <sup>4</sup>Institute of Geology of Ore Deposits, Petrography, Mineralogy, and Geochemistry, Moscow, Russia, <sup>5</sup>Volcanic Basin Petroleum Research, Oslo, Norway

## OPEN ACCESS

### Edited by:

Chiara Maria Petrone,  
Natural History Museum,  
United Kingdom

### Reviewed by:

Stephen Self,  
University of California Berkeley,  
United States  
Mark Kendrick,  
The University of Queensland,  
Australia

### \*Correspondence:

Marie Edmonds  
marie.edmonds@esc.cam.ac.uk

### Specialty section:

This article was submitted to  
Petrology,  
a section of the journal  
Frontiers in Earth Science

**Received:** 14 July 2021

**Accepted:** 20 August 2021

**Published:** 09 September 2021

### Citation:

Sibik S, Edmonds M, Villemant B, Svensen HH, Polozov AG and Planke S (2021) Halogen Enrichment of Siberian Traps Magmas During Interaction With Evaporites. *Front. Earth Sci.* 9:741447. doi: 10.3389/feart.2021.741447

Volatile emissions to the atmosphere associated with the Siberian Traps eruptions at the Permian-Triassic boundary were sourced from the outgassing of primary magmas and the sedimentary host rocks into which they were intruded. Halogens in volcanic gases may have played an important role in environmental degradation and in stratospheric ozone destruction. Here we investigate how halogens behave during the interaction between salts and basalt magma emplaced as sills and erupted as lava. We present whole-rock, trace, and halogen concentrations for a suite of samples from three locations in the Siberian Traps Large Igneous Province, including basalt lavas erupted, and dolerites intruded into both organic-bearing shales and evaporites. Dolerites are enriched in Cl, Br, and I; their enrichment in Cl is similar to MORB and OIB that have been inferred to have assimilated seawater. The dolerites exhibit halogen compositional systematics, which extend towards both evaporites and crustal brines. Furthermore, all analyzed samples show enrichment in Rb/Nb; with the dolerites also showing enrichment in Cl/K similar to MORB and OIB that have been inferred to have assimilated seawater. We infer that samples from all three locations have assimilated fluids derived from evaporites, which are components of crustal sedimentary rocks. We show that up to 89% of the chlorine in the dolerites may have been assimilated as a consequence of the contact metamorphism of evaporites. We show, by thermal modeling, that halogen transfer may occur via assimilation of a brine phase derived from heating evaporites. Halogen assimilation from subcropping evaporites may be pervasive in the Siberian Traps Large Igneous Province and is expected to have enhanced emissions of Cl and Br into the atmosphere from both intrusive and extrusive magmatism.

**Keywords:** Siberian Traps, halogens, degassing, contact metamorphism, magma

## INTRODUCTION

The Siberian Traps Large Igneous Province, now thought to have been emplaced rapidly within  $60 \pm 48$  ka at the end of the Permian (Reichow et al., 2009; Burgess et al., 2014; Shen et al., 2019), was synchronous with the largest mass extinction in Earth's history (Renne and Basu, 1991; Renne et al., 1995; Burgess et al., 2017). There remains much controversy about the mass extinction mechanism, but there is a consensus that outgassing of volatiles was a primary environmental perturbation agent

(Campbell et al., 1992; Lomax et al., 2005; Self et al., 2005; Beerling et al., 2007; Black et al., 2012). Carbon-, sulfur- and halogen-bearing gas species all have the potential to affect the environment in ways that could be significant enough to cause environmental degradation and impact life on Earth. Emissions of carbon gases (CO<sub>2</sub> and CH<sub>4</sub>) were caused by the devolatilization of carbon-rich shales, coal, and evaporites due to heating from sill intrusions (Svensen et al., 2009), as well as from the outgassing of ascending and erupting magmas (Self et al., 2005; Black et al., 2012). These emissions may have led to significant perturbations to the carbon budget, leading to ocean warming and anoxia, with implications for biological productivity and life (Payne et al., 2004). The long-term warming caused by carbon emissions might have been punctuated by short-term (10–100 years) cooling due to sulfate aerosol formation in the troposphere (Self et al., 2005), which might have persisted to varying degrees throughout the Siberian Traps eruptions (Black et al., 2018). Acid rain affected both terrestrial and ocean environments, promoting weathering and ocean acidification (Black et al., 2014). Methane may have been generated from methanogenic microorganisms in the oceans, activated by nickel (Rothman et al., 2014; Le Vaillant et al., 2017), perhaps transported to the marine environment via sulfate aerosols during Siberian Traps eruptions (Rampino et al., 2017). In addition, it has been suggested that the mantle source feeding the Siberian Traps volcanism was fundamentally rich in carbon and chlorine from recycled oceanic crust that had been inefficiently devolatilized during subduction (Sobolev et al., 2011; Sibik et al., 2015; Broadley et al., 2018). Magma outgassing during emplacement in the crust and during eruption would have transferred these volatiles to the atmosphere.

Halogen outgassing systematics during Siberian Traps Large Igneous Province formation is not well understood. It has been suggested that organohalogens emitted from the Siberian Traps magmas and the country rocks may have been a significant factor in causing mutations and damaging the DNA of life via enhanced UVB radiation fluxes (Beerling et al., 2007; Svensen et al., 2009; Benca et al., 2018). Halogen-bearing gas species, once in the atmosphere, can be converted into the reactive molecules chlorine monoxide (ClO) and bromine monoxide (BrO); and chlorine and bromine atoms (Cl and Br) (Oppenheimer et al., 2006). These species readily enter into self-sustaining ozone destruction reactions (Bobrowski et al., 2003; Gerlach, 2004). Bromine free radicals are 40–70 times more efficient in damaging the ozone layer than chlorine free radicals (Daniel et al., 1999; Sinnhuber et al., 2009); and the destructive potential of bromine is enhanced when accompanied by stratospheric sulfate aerosol loading, which is particularly relevant for an evaluation of the Siberian Traps eruption's climatic effects.

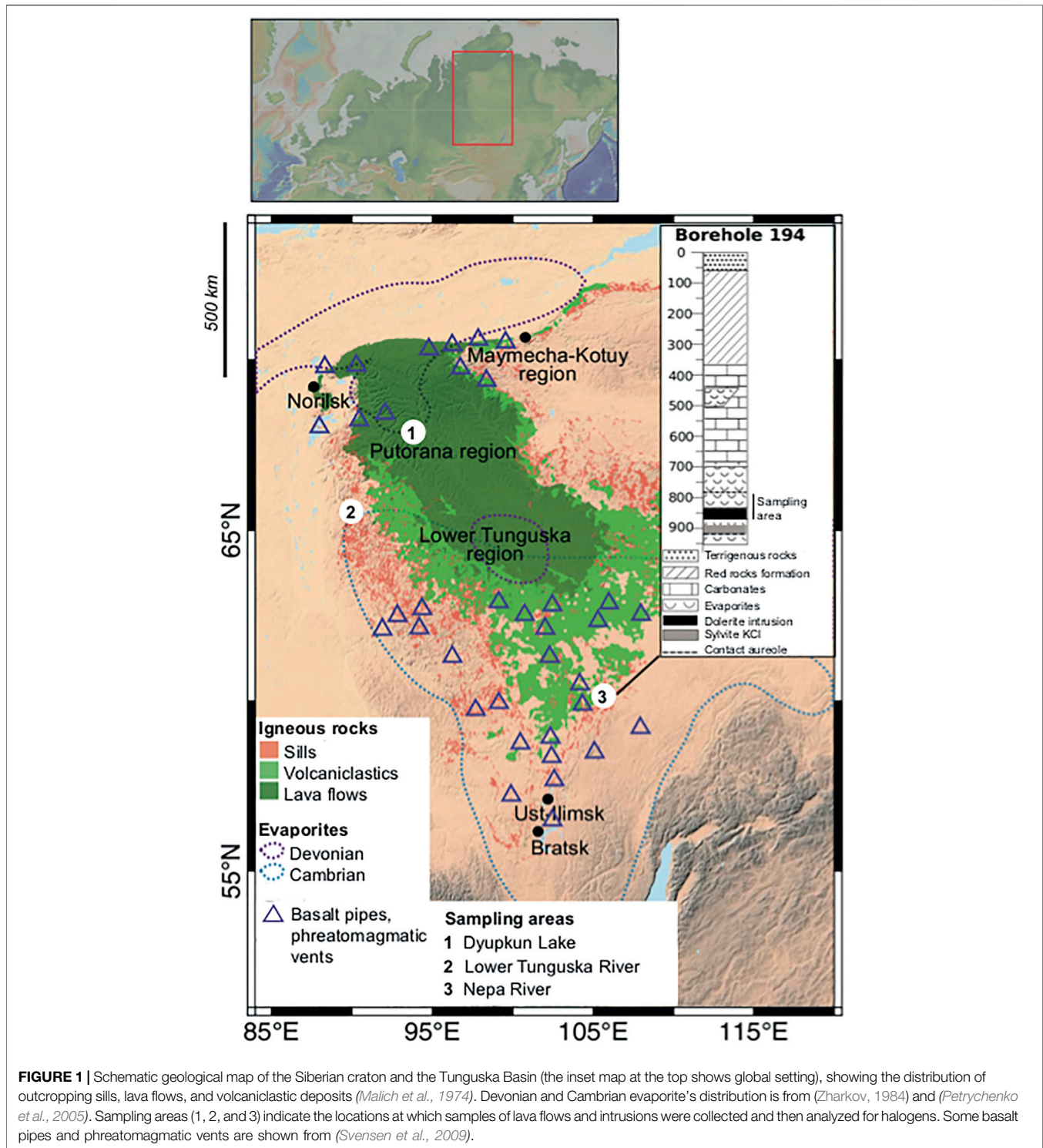
Despite the importance of halogen outgassing for atmospheric chemistry and the atmosphere's radiation budget, unequivocal geochemical evidence for their origin and outgassing mechanism during the Siberian Traps eruptions remains elusive. The Cambrian and Devonian age evaporites dominate in the southern and northern parts, respectively, of the Siberian craton sedimentary sequence (**Figure 1**). Sills comprise a

significant volume of the Siberian Traps Large Igneous Province (between 37 and 44%) (Vasil'ev et al., 2000). Most of the lavas and sills on the craton were emplaced in a region of subcropping Devonian evaporites, mainly composed of sulfates (in the thick upper and lower parts) and halite (in the middle part) (Zharkov, 1984). Cambrian evaporites are composed of salts (dominated by halite) and proposed to be volatilized in areas adjacent to sills (Svensen et al., 2009; Svensen et al., 2018). Interactions between magmas and evaporites, including the incorporation of sedimentary pore fluids (e.g., brines), can significantly increase the volatile contents of magmas (Heimdal et al., 2019), as has been suggested to explain some high chlorine contents of melt inclusions in Siberian Traps Large Igneous Province rocks (Sobolev et al., 2009; Black et al., 2012). Previous studies have described the textures and skarn mineralogy produced at the contact between dolerites and evaporites in the Nepa River region (Grishina et al., 1991; Grishina et al., 1992; Istomin et al., 2000; Mazurov et al., 2007; Polozov et al., 2016; Grishina et al., 2018; Grishina et al., 2020). Evidence for interactions with magmas may be retained in the basalts and the contact aureole in the salts. However, the analytical challenges associated with the measurement of bulk rock halogens have, up to now, largely prevented close examination. More than 500 basaltic phreatomagmatic and ~250 magnetite-rich breccia pipes are found in the Siberian Traps LIP (Svensen et al., 2009; Polozov et al., 2016), **Figure 1**). These magmatic breccia pipes likely played a vital role in the liberation of halogens to the atmosphere (Svensen et al., 2009; Aarnes et al., 2010; Polozov et al., 2016).

In this paper, we present whole-rock halogen compositions in a magma-sediment system from the Siberian Traps Large Igneous Province to assess the extent to which halogens have been assimilated into the magmas and outgassed from the surrounding salts; and the mechanisms by which this occurred. We present the results of a detailed geochemical investigation of both dolerite sills and basaltic lava flows emplaced in different basin segments (Dyupkun Lake, Lower Tunguska River and the Nepa River; **Figure 1**) with the lower parts dominated by evaporites including salt and dolostones (location 3, Nepa River, "NP-43"-series samples; **Figure 1**), and the shallow parts dominated by carbonates and siliciclastic rocks (locations 1 and 2, Dyupkun Lake and Lower Tunguska River, "S10"-series samples; **Figure 1**), including thick coal beds. We discuss the influence of these halogen-rich enclosing sedimentary rocks on magma geochemistry and the volatile budget of the Siberian Traps Large Igneous Province eruptions.

## SAMPLES AND METHODS

The samples of lavas and sills, including sampling coordinates, are provided in the **Supplementary Material**; the sampling locations are shown in **Figure 1**. Petrological descriptions of the S10 series at locations 1 and 2 on the map are provided by Sibik et al. (2015), except for the two samples S10-49 and S10-58. The sill and enclosing salt samples from location 3 on the map ("NP"-series, **Supplementary Material**) are first described in this



study. Samples from location 1 are basalt flows of the Ayanskaya Formation at Dyupkun Lake (Putorana Plateau), which were emplaced on Cambrian-Silurian carbonate and terrigenous strata, Devonian evaporites with rock salts, and Carboniferous-Permian terrigenous coal-bearing strata and erupted onto basalts of Tutonchana Horizon. Samples of location 2 are dolerite sills in

the Lower Tunguska River region which travelled through Cambrian evaporites with anhydrite, Ordovician-Devonian carbonate terrigenous strata, and were emplaced into Carboniferous-Permian organic-rich shales and coal-bearing strata. Samples of location 3 are from a 40-m thick dolerite sill crossed by borehole 194 in the Nepa River region (inset, **Figure 1**;

coordinates N59°9'20" E107°37'2"). This dolerite sill intruded into the salt horizon of the Lower Cambrian evaporites (mostly halite, but also potassium salts) and was sampled from the middle part of intrusion downward to the footwall contact. Dolerite mineralogy comprises clinopyroxene and plagioclase with frequent olivine, as described by Sibik et al. (2015).

Whole-rock major and trace element compositions of lava flows and intrusions from Dyupkun Lake and Lower Tunguska River regions were obtained using combined ICP-MS and ICP-AES analyses (Sibik et al., 2015) (see **Supplementary Material** for detail of analytical methods). Major and trace elements for the "NP"-series were analyzed at the University of Cambridge (United Kingdom) by ICP-MS. Before halogen analysis, the small amounts (~1.7–2 g) of finely powdered dolerites were mixed with ~20 ml distilled water. The mixtures were then heated to 70°C to dissolve the dolerite-impregnated salts. This procedure was repeated three times to ensure complete removal of salt material, and then the powders were dried in the oven.

Fine powders of 12 samples of pre-washed dolerites and basalts (**Figure 1**) were analyzed for halogens at the Alipp6 laboratory, ISTEP, Sorbonne Université, Paris, France. Rock powders underwent pyrohydrolysis for halogen extraction: 1 g of the sample powder was mixed with an excess of vanadium pentoxide and then placed in a platinum crucible. It was heated in a combustion tube to 1,200°C through water vapor-stream transported by a nitrogen flux. Water vapor containing halogens was condensed by a cooling system and trapped in sodium hydroxide (Michel and Villemant, 2003) followed by Ion Chromatography (IC). The solutions obtained by pyrohydrolysis, the leachates, and dissolved host evaporites from location 3 were analyzed by Ion Chromatography (IC) for chlorine and fluorine and by Inductively-Coupled Plasma Mass Spectrometry (ICP-MS) on a PerkinElmer SCIEX Elan DRC II quadrupole ICP-MS system for bromine and iodine. Fine powders were analyzed for trace elements: 0.1 g of powder was digested in screw-capped PFA (Teflon) containers using the HF-HNO<sub>3</sub> technique (Jarvis and Jarvis, 1992) and Evapoclean system for heating and evaporation. The final solution was then diluted by up to 50 ml volume to 2% HNO<sub>3</sub>. Instrument calibration was performed using international rock standards BCR-2 and BHVO-2 and in-house standards to monitor In, Re, and Rh drift. The measurement's precision, based on the standard deviation of repeat analysis of standard materials, is 7% for fluorine, 11% for chlorine, 15% for bromine, 57% for iodine, and less than 4% for typical trace elements.

## RESULTS

The compositions of lava flows and sills erupted onto or intruded into siliceous continental crust (locations 1 and 2 on **Figure 1**, samples "S10"-series) and of dolerite sills emplaced in evaporites in the Nepa region (location 3 on **Figure 1**, samples "NP-43"-series) are reported in **Supplementary Material** and in **Table 1**. The major element compositions of the samples plot directly onto the liquid line of descent defined by previous studies of Siberian traps volcanic and plutonic rocks (Hawkesworth et al., 1995; Fedorenko and Czamanske, 1997; Czamanske et al., 2000) and do

not show any anomalous enrichment in alkali elements (**Supplementary Material Figure S2**).

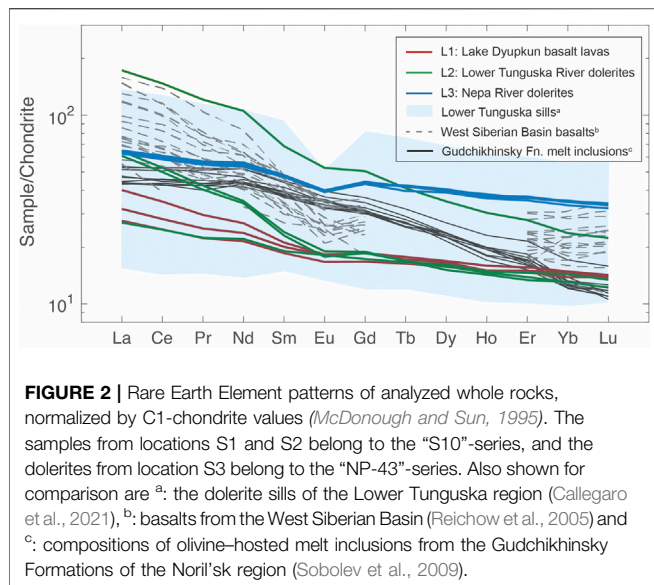
The Rare Earth Element (REE) chondrite-normalized compositions are shown in **Figure 2**, shown alongside whole rock basalt compositions from the West Siberian Basin (Reichow et al., 2005) and olivine-hosted melt inclusions from the Gudchikhinsky Formation (Sobolev et al., 2009). Sample S10-49 is more evolved than other samples of the S10-series, with a MgO content of 3.58 wt% compared to 6.93–7.81 wt% for the other S10 series rocks; and higher K<sub>2</sub>O contents (1.82 against 0.14–1.08 wt%) and significantly higher concentrations of incompatible trace elements (**Supplementary Material; Figure 2**). Sample S10-49 has a higher La/Yb ratio (10.73) compared to the La/Yb range of 2.77–7.26 in other S10-series magmas. Other S10-series magmas have a variable La/Sm (2.27–4.28) ratio at nearly the same Sm/Yb (1.22–1.70) except the S10-49 sample, which has a Sm/Yb ratio of 2.65.

The basalts and dolerites contain variable concentrations of chlorine (up to 5,331 ppm), bromine (0.44–5.89 ppm), iodine (up to 205 ppb), and fluorine (171–983 ppm) (**Table 1; Figure 3, Supplementary Material Figure S3**). The basalts erupted onto the siliceous continental crust (location 1) have much lower concentrations of chlorine (< 150 ppm) than the dolerites from location 2, as well as slightly lower fluorine (< 210 ppm compared with 210–990 ppm), bromine (< 1.0 as opposed to 1–1.4 ppm) and similar iodine concentrations (up to 44 and 67 ppb correspondingly). Sample S10-49 (location 2) contains the highest concentrations of F (983 ppm), Cl (5,331 ppm). In contrast, sample S10-44 (location 2) contains the lowest concentration of F (213 ppm) and Cl (325 ppm) within the range of location 2 dolerites (**Table 1; Figure 3**). When plotted against MgO contents, it can be seen that the Cl contents of the whole rock samples increases with decreasing MgO content (**Supplementary Material Figure S3**), similar to published melt inclusion compositions (Sobolev et al., 2009; Black et al., 2012). There is no clear relationship between the Cl and Na<sub>2</sub>O or K<sub>2</sub>O contents of the rocks, as might be expected for fractionation trends, and the Cl/K<sub>2</sub>O ratio of 0.33 (derived from a regression through the data in this study) is much larger than the upper limit of 0.06 observed in mid-ocean ridge basalts (Michael and Cornell, 1998). Indeed, there is a very large spread in whole rock and melt inclusion Cl contents over a relatively small range in Na<sub>2</sub>O and K<sub>2</sub>O contents, which is not consistent with a fractionation trend (**Supplementary Material Figure S3**).

The halogen concentrations measured in MORB and OIB are also shown in **Figure 3** together with mantle Br/Cl and I/Cl ranges (black, dashed lines) and suggested mantle F/Cl ratios (Kendrick et al., 2020). On a fluorine - chlorine plot (**Figure 3A**), only basalts from location 1 plot in the MORB field, which is itself not precisely determined (Kendrick et al., 2017). In contrast, all of the dolerites (locations 2 and 3) are chlorine-enriched and plot close to MORB glass inferred to have assimilated seawater Cl (Kendrick et al., 2017). On a bromine—chlorine plot (**Figure 3B**), all of the basalts and dolerites are outside the mantle range (Br/Cl =  $2.8 \pm 0.6 \times 10^3$ ) (Kendrick et al., 2017). All of the basalts from location 1 and one dolerite (S10-44 of location 2) are slightly Br-enriched (or Cl-depleted); in contrast, all of the other

**TABLE 1** | Whole rock compositions, including major, trace and halogens, of the rocks analyzed in this study. Methods are described in the text and in the **Supplementary Material**. Locations from which the samples are derived are at the top of the table, as well as sampling height (metres) for the dolerites from location 3, borehole 195.

Sampling Ht	Location 1, Dyupkun Lake basalts			Location 2, Lower Tunguska River dolerites				Location 3, Nepa River dolerites				
	S10-12	S10-15	S10-22	S10-44	S10-49	S10-58	S10-62	864.3 m NP-9843	879.2 m NP-9845	879.2 m NP-9847	879.2 m NP-9848	885.9 m NP-9850
<b>Major elements</b>												
MgO	7.47	7.70	7.37	7.81	3.58	6.93	6.94	4.09	3.88	4.06	4.07	4.08
MnO	0.18	0.18	0.16	0.19	0.22	0.17	0.16	0.3	0.29	0.29	0.3	0.3
Al <sub>2</sub> O <sub>3</sub>	15.9	15.6	15.3	16.0	13.0	15.4	15.9	11.7	11.1	11.5	11.4	11.7
CaO	11.5	12.0	11.6	10.4	7.56	11.1	11.3	9.20	8.75	8.91	8.82	9.05
TiO <sub>2</sub>	1.11	1.03	1.06	1.12	3.26	0.94	0.93	2.71	3.22	2.91	2.87	2.91
Na <sub>2</sub> O	2.12	2.01	2.08	2.22	3.33	1.97	2.34	2.65	2.51	2.73	2.62	2.63
K <sub>2</sub> O	0.21	0.14	0.32	0.43	1.82	1.08	0.96	0.94	0.93	1.00	0.99	1.02
P <sub>2</sub> O <sub>5</sub>	0.13	0.11	0.11	0.12	0.79	0.10	0.10	0.31	0.31	0.31	0.30	0.32
<b>Trace elements</b>												
Li	21.8	7.68	4.99	12.7	36.1	22.8	22	19.6	13.7	17.0	16.4	35.3
Be	0.54	0.48	0.60	0.41	1.68	0.86	0.88	1.1	1.3	1.0	1.0	1.1
Sc	44.4	46.2	44.4	39.8	32.9	38.9	37.8	53.2	54.3	54.2	53.6	53.7
V	321	323	320	301	273	270	267	520	624	568	554	567
Cr	126	147	130	131	11.1	62.3	64.8	17.2	12.6	14.5	15.2	13.2
Co	50.3	50.2	48.1	53.0	32.6	39.6	40.4	51.6	49.5	49.0	49.7	50.4
Ni	114	119	84.6	136	10.6	12.0	11.9	25.4	22.4	22.4	23.1	23.5
Cu	125	122	108	124	42.6	20.8	20.7	348	356	351	333	361
Zn	88.7	80.1	83.8	104	114	50.3	51.6	163	144	187	156	201
Ga	17.2	17.0	16.9	17.3	23.4	17.0	17.3	24.0	24.2	23.6	23.6	24.4
Rb	7.68	2.20	5.44	12.0	76.3	44.1	41.8	26.6	21.0	29.8	24.2	29.5
Sr	210	193	217	218	392	231	253	224	209	200	205	210
Y	24.5	22.7	22.9	22.6	46.1	21.8	22.3	54.7	55.9	57.4	56.7	57.6
Zr	81.7	78.0	93.0	70.4	272.4	105.3	106	198	213	202	203	205
Nb	4.55	3.76	5.14	3.81	23.6	6.64	6.68	9.81	10.8	10.2	10.1	10.1
Sn	0.73	0.68	0.75	0.73	1.09	0.91	0.62	1.84	1.59	2.04	1.65	2.09
Cs	0.30	0.19	0.42	0.50	2.29	2.34	2.20	0.52	0.36	0.87	0.60	0.88
Ba	111	124	160	143	503	255	184	248	200	214	212	224
La	7.56	6.54	9.50	6.39	41.0	14.4	15.2	14.8	15.3	15.0	15.1	15.4
Ce	17.3	15.2	21.4	15.2	90.4	30.6	32.3	35.8	36.8	36.6	36.2	37.4
Pr	2.33	2.07	2.75	2.08	11.2	3.74	3.93	5.07	5.20	5.18	5.15	5.28
Nd	10.9	9.82	12.2	10.1	48.2	15.6	16.1	24.3	25.4	25.2	24.9	25.7
Sm	2.97	2.75	3.13	2.82	10.1	3.41	3.56	6.95	7.06	7.11	6.97	7.12
Eu	1.02	0.94	1.03	1.02	2.96	1.00	1.07	2.21	2.24	2.22	2.20	2.25
Gd	3.70	3.33	3.69	3.44	10.1	3.70	3.76	8.59	8.69	8.61	8.61	8.83
Tb	0.64	0.59	0.62	0.60	1.48	0.61	0.61	1.43	1.51	1.53	1.51	1.51
Dy	4.15	3.87	4.08	3.98	8.60	3.72	3.88	9.58	9.84	9.96	9.76	9.87
Ho	0.87	0.82	0.82	0.81	1.66	0.78	0.8	1.98	2.08	2.05	2.02	2.05
Er	2.50	2.35	2.40	2.34	4.45	2.14	2.22	5.66	5.82	5.93	5.83	5.89
Tm	0.38	0.35	0.36	0.35	0.63	0.33	0.33	0.85	0.89	0.90	0.89	0.88
Yb	2.39	2.23	2.35	2.31	3.82	2.10	2.10	5.37	5.68	5.64	5.59	5.58
Lu	0.35	0.34	0.34	0.33	0.55	0.30	0.30	0.79	0.83	0.84	0.83	0.82
Hf	2.37	2.05	2.43	1.99	6.70	2.77	2.74	5.26	5.69	5.51	5.41	5.45
Ta	0.28	0.23	0.32	0.24	1.38	0.40	0.41	0.61	0.66	0.64	0.61	0.64
Tl	0.07	0.05	0.04	0.06	0.18	0.24	0.17	0.09	0.06	0.13	0.10	0.15
Pb	8.47	2.06	11.97	2.41	4.41	2.67	2.17	1.96	1.35	4.25	2.32	6.16
Th	1.19	1.05	1.71	0.91	4.99	2.80	2.88	2.04	2.09	2.09	2.02	2.09
U	0.52	0.43	0.59	0.38	1.21	0.83	0.84	0.91	0.95	0.93	0.91	0.92
<b>Halogens</b>												
F, ppm	204	171	209	213	983	317	298	480	400	459	343	549
Cl, ppm	92	151	63	325	5331	1569	2068	3022	1852	4143	2307	3675
Br, ppb	400	1000	500	1400	1300	1000	1400	3900	4000	4400	2800	5900
I, ppb	19	44	1	65	11	15	67	63	12	205	21	101
F/Cl	2.2	1.1	3.3	0.66	0.18	0.20	0.14	0.16	0.22	0.11	0.15	0.15
Br/Cl (x 10 <sup>3</sup> )	4.3	6.6	7.9	4.3	0.24	0.64	0.68	1.3	2.2	1.1	1.2	1.6
I/Cl (x 10 <sup>6</sup> )	210	290	16	200	2.1	9.6	32	21	6.5	50	9.1	27



dolerites (locations 2 and 3; **Figure 1**) are Cl-enriched (or Br-depleted). On an iodine—chlorine plot (**Figure 3C**), again almost all of the studied basalts and dolerites plot outside of the mantle range ( $I/Cl = 60 \pm 30 \times 10^6$ ) (Kendrick et al., 2017). Two basalts (from location 1) and one dolerite (S10-44 of location 2) are I-enriched (or Cl-depleted), whereas all other dolerites (from locations 2 and 3) are Cl-enriched (or I-depleted). Three dolerites from location 3 (the Nepa River region) and one dolerite from location 2 (S10-62, the Lower Tunguska River) have an I/Cl ratio that almost coincides with the mantle but lies far from mantle Br/Cl values. However, these samples coincide with the field for MORB and OIB glasses inferred to have assimilated seawater Cl (Kendrick et al., 2017). As a whole, there is enrichment in Cl, and to some extent, Br and I over MORB values observed for both dolerites intruded into evaporites (location 3) and into siliceous continental crust (location 2). On a I/Cl vs Br/Cl plot (**Figure 3D**), all dolerites and basalts plot significantly outside the mantle field and are dispersed between the endmember compositions of evaporites, seawater, and crustal brines (Kendrick et al. (2017)). The borehole 194 samples display a lower I/Cl ratio than “typical” evaporites (Zherebtsova and Volkova, 1966; McCaffrey et al., 1987; Kendrick et al., 2017); the I content of the Nepa evaporites is below detection (**Table 2**). Sedimentary evaporites of the Nepa River area have the lowest values of I/Cl, with iodine contents close to the limit of detection.

The stratigraphy of the sill intruded into salts (inset in **Figure 1**) is illustrated in **Figure 4** with the halogen and sulfur concentrations measured in this study. The halogen analysis of leachates from the purification of sill samples intruded into salts (NP-43), and the chlorine, bromine, iodine, and sulfur concentrations in both dolerite (**Table 1**) and evaporite (**Table 2**) lithologies are also shown. There are considerable fluctuations in chlorine concentrations in the evaporites on the bottom contact with the sill; above the sill, the lowest chlorine concentrations are found near the contact. Bromine

concentrations in the evaporites increase towards the contact with the sill on both sides of the intrusion, but particularly towards the lower contact, from 122 ppm 61 m from the contact to 869 ppm 1.5 m from the contact, which results in an increase in Br/Cl from  $0.22 \times 10^3$  to  $1.38 \times 10^3$  (**Figure 4**; **Table 2**). Iodine is present at higher concentrations in the sill than in the adjacent sedimentary rocks (**Figure 4**). The evaporite samples are depleted in I (relative to Cl) compared to “typical” evaporites (**Figures 3D**; **Figure 4**).

Trace element ratios and chlorine contents for the studied magmatic rocks are plotted in **Figure 5**. All the dolerite samples have a La/Yb ratio similar to MORB and OIB basalt glasses, but they are Cl-enriched compared to MORB and OIB (except one; S10-44; **Figure 5A**). On a plot of Cl/K vs Rb/Nb (Asafov et al., 2020) all dolerite and basalt samples plot outside the field of MORB and OIB basalt glasses (Kendrick et al., 2017) and are shifted to higher Rb/Nb ratios except for one basalt sample (S10-15) that has the lowest Rb (2.2 ppm) content and coincides with the field of reference samples inferred to have assimilated seawater Cl. All studied samples form a generally positive array on the Cl/K vs Rb/Nb plot (**Figure 5B**).

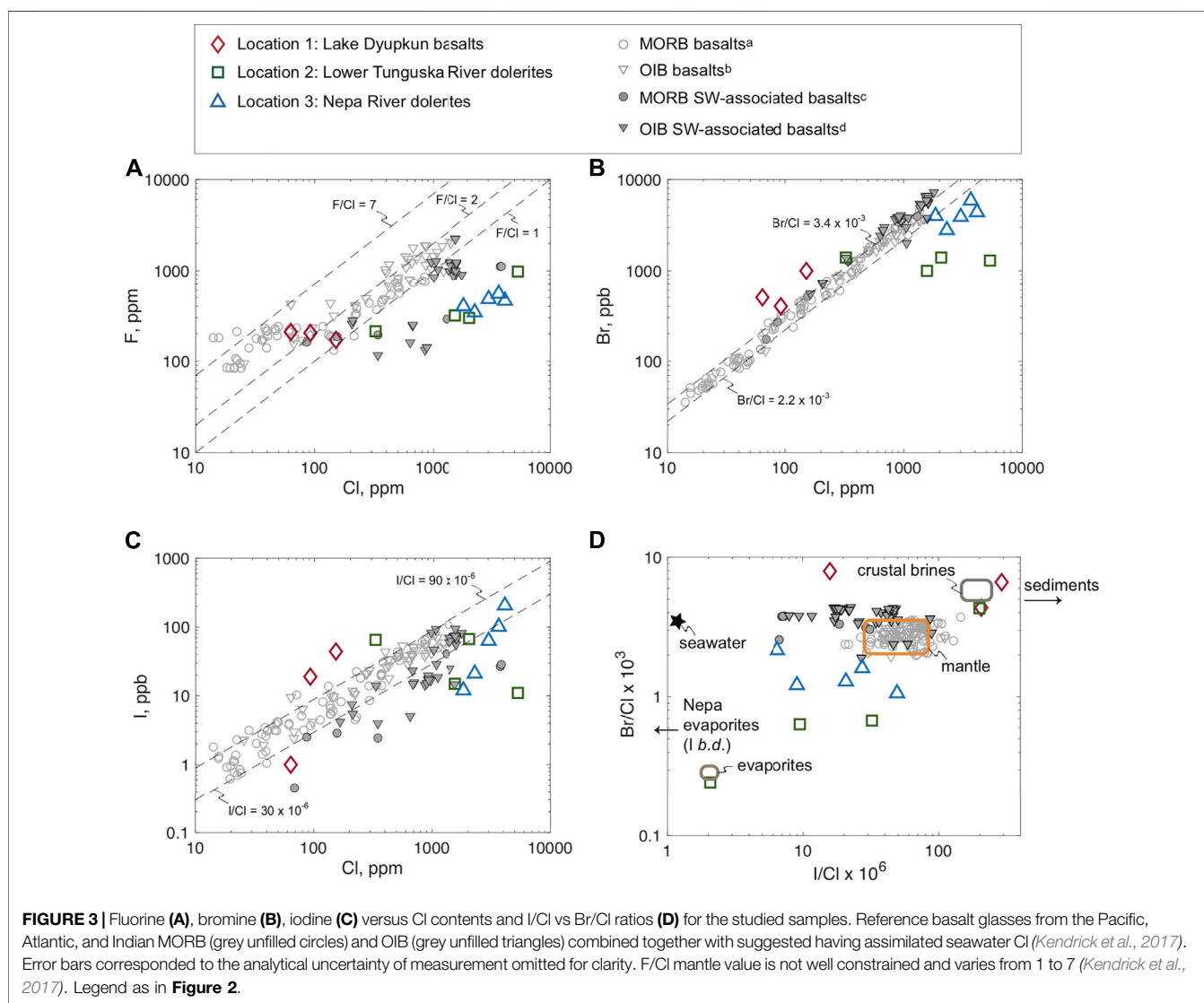
## DISCUSSION

### Origin of Halogens in Basalts and Dolerites of the Siberian Traps Large Igneous Province

Halogens are expected to behave similarly to incompatible elements during mantle melting, and crystallization. The fluorine and chlorine concentrations in the basalts increase with La/Yb for MORB and OIB melts uncontaminated with seawater chlorine (Kendrick et al., 2012) (**Figure 5A**); thus mantle melts with high La/Yb, are expected to be Cl-rich (**Figure 5A**). As they are all similarly incompatible, the ratios between the halogens do not change significantly during melting or fractionation. These ratios reflect the abundances of the halogens in the MORB-OIB mantle source uncontaminated by seawater (Kendrick et al., 2012). Some OIB glasses proposed to be contaminated with seawater do not demonstrate Cl-enrichment beyond what is expected for their La/Yb ratio (**Figure 5A**). In contrast, all seawater-contaminated MORB glasses, some contaminated OIB glasses, and almost all studied dolerites of the Siberian Traps are demonstrably Cl-enriched (**Figure 5A**). Chlorine enrichment for the seawater-contaminated MORB-OIB glasses can also be seen on the Cl/K vs Rb/Nb plot (**Figure 5B**). However, unlike seawater-contaminated MORB and OIB, all of the Siberian basalts and dolerites, except one, are shifted from the cloud of MORB-OIB mantle melts towards high Rb/Nb, with less significant Cl/K enrichment. We note that olivine-hosted melt inclusions from the Gudchikhinsky Formation (Sobolev et al., 2009) also show a correlation between Cl/K and Rb/Nb and extend to the same region of the plot in **Figure 5B**. We propose that the trends towards high Cl and LILE exhibited by the Siberian Traps Large Igneous Province magmas from all three locations studied here are

**TABLE 2 |** Whole rock compositions of evaporite samples from the Nepa River borehole 194 measured in this study (methods described in main text and in the **Supplementary Material**). Sample names are given in the first column. The distance from the contact with the dolerite, in meters, is given for evaporites above the upper contact with the dolerite, and below the lower contact, along with sampling height in the borehole. The halogen compositions are given in parts per million (ppm). Note that the iodine composition of the evaporite samples is at or below detection, which is 5 ppb (parts per billion).

	Distance from contact, m	Sampling height in the borehole, m	F, ppm	Cl ( $\times 10^3$ ) ppm	Br, ppm	I, ppb	S, ppm	Br/Cl ( $\times 10^3$ )	I/Cl ( $\times 10^6$ )
Above upper contact									
NP 9835	79.5	765.5	b.d.	930	302	5	3596	0.32	5.38
NP 9828	4	841	b.d.	547	329	5	313	0.60	9.14
NP 9859	0.4	844.6	229	606	477	5	229	0.79	8.25
Below lower contact with dolerite									
NP 9852	1.5	886.2	252	629	869	5	2323	1.38	7.95
NP 9838	9	889.8	b.d.	536	702	5	4033	1.31	9.33
NP 9861	27.4	904.2	b.d.	795	515	5	697	0.65	6.29
NP 9854	61	915.7	269	550	122	5	406	0.22	9.09



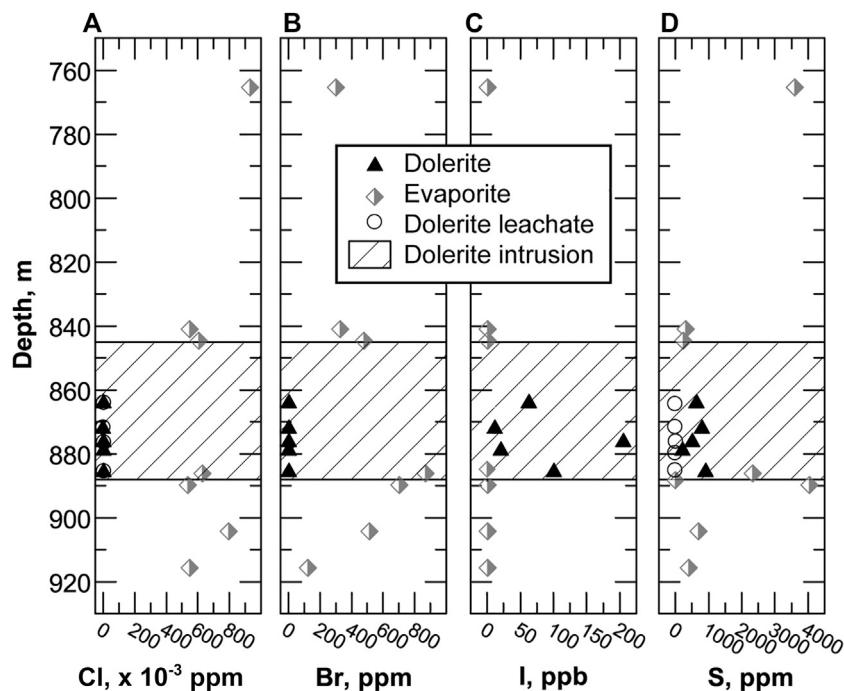


**FIGURE 4** | Stratigraphic sections through the borehole to show (A) chlorine, in ppm; (B) bromine (C) iodine and (D) sulfur compositional variations through the enclosing evaporites and intruded dolerite sill across the borehole 194.

caused by varying degrees of assimilation of crustal sedimentary rocks (including evaporites) by the Siberian Traps magmas during their emplacement, as has been suggested by others (Lightfoot et al., 1990; Wooden et al., 1993; Callegaro et al., 2021).

In some basalts/dolerites (those from locations 1 and 2) (Figure 3) bromine and, to a lesser extent, iodine are at higher values than MORB-OIB basalts with their F/Cl ratio close to the mantle range 1–7 (Kendrick et al., 2017). The Br/Cl ratio for all basalts and one dolerite (S10-44) exceeds those of mantle melts (determined as  $2.8 \pm 0.6 \times 10^{-3}$  by Kendrick et al.,

2017) (Figure 3B), and plot close to seawater–crustal brines–sedimentary rocks compositions (Figure 3D). All other dolerites (from locations 2 and 3) intruded into the terrigenous crustal rocks and evaporites are Cl-enriched and plot close to seawater–evaporite compositions (Figure 3D). These deviations in halogen compositions from MORB-OIB basalts are not consistent with degassing from evolved, uncontaminated magmas. Instead, we suggest that the enrichment in Cl and mobile elements (as represented by Rb) is due to the magmas passing through sedimentary strata containing evaporites, which are present at all of the studied localities (Figure 1). Here we note that the halogen systematics of these samples (largely extending to lower Br/Cl than the mantle and towards evaporite compositions; Figure 3D); are not consistent with their having interacted with a postulated high Br/Cl sub-continental lithosphere, as has been previously proposed as a potential halogen source (Broadley et al., 2018). It is very likely that in our sample set, and perhaps other published sample sets, we have no halogen-uncontaminated Siberian Traps rocks; thus, it is not possible to estimate the Siberian Trap's primary halogen contents based on the current samples. It is likely that halogens are held in the form of halogen-bearing minerals (apatite, mica, amphibole) in the dolerites, although this requires further detailed microanalysis and imaging. The pipes in the Siberian Traps, for instance at Nepa, contain abundant and halogen-rich apatite (Neumann et al., 2017).

The basalts from location 1 (Lake Dyupkun) are subaerial lavas, and are relatively depleted in Cl relative to the dolerite samples from locations 2 (Lower Tunguska) and 3 (Nepa River)

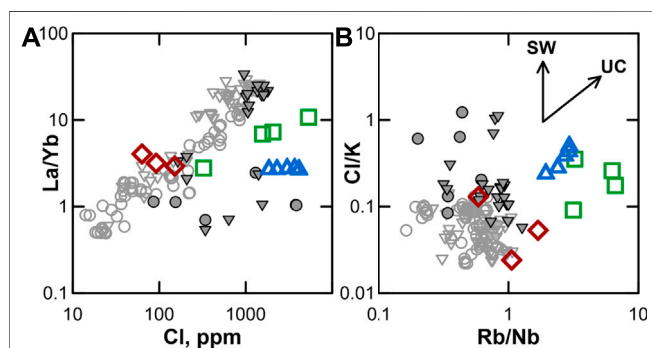


**FIGURE 5** | (A) La/Yb versus Cl and (B) Cl/K vs Rb/Nb ratios for studied dolerites and basalts (Asafov et al., 2020). The values of MORB and OIB reference glasses are after Kendrick et al. (2017). SW and UC trends (b) denote seawater or upper crust assimilation, respectively. Legend as in Figure 2.

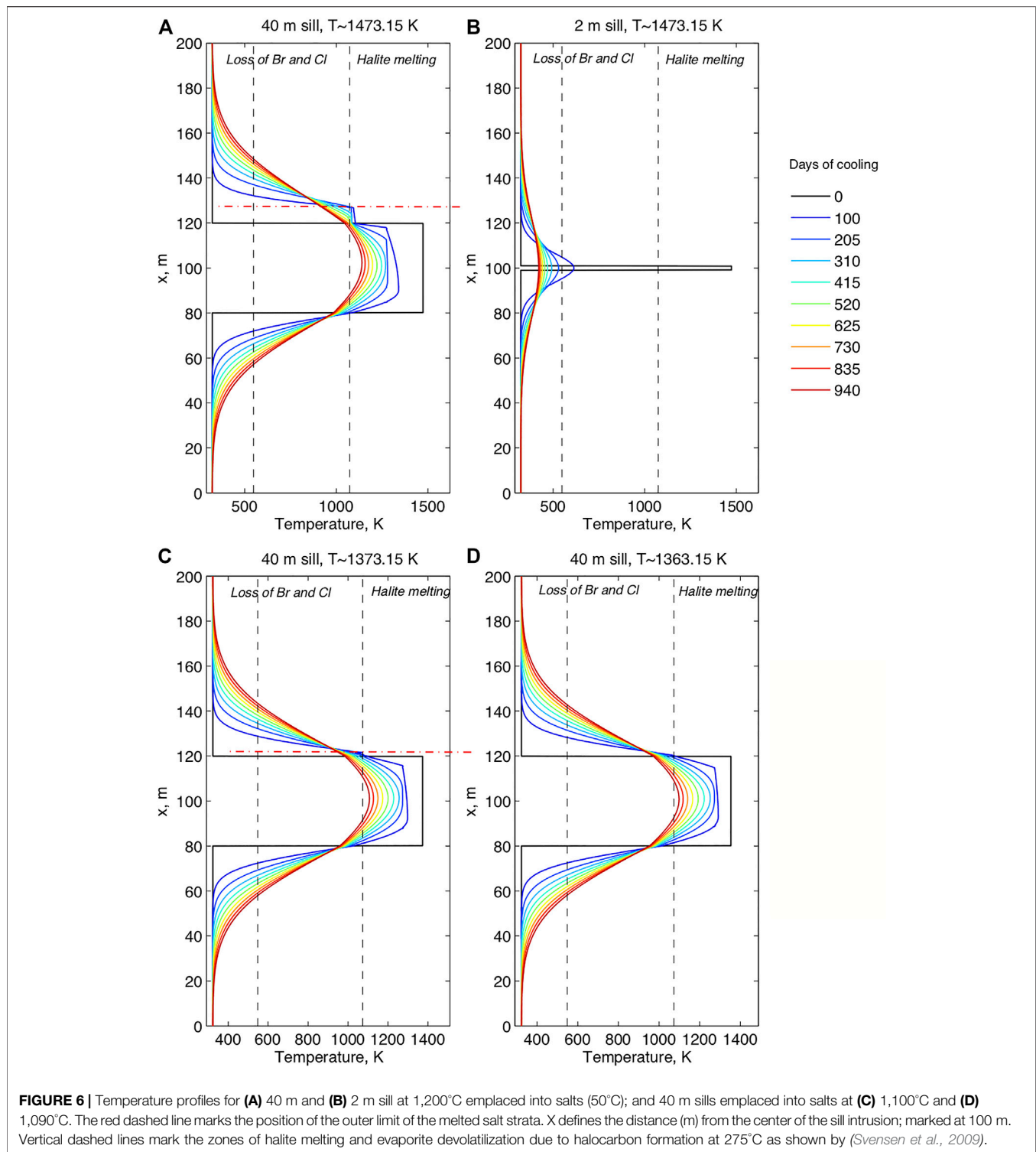


(Figure 3; Supplementary Material Figure S3). The basalts from location 1 are more primitive than those from locations 2 and 3, although there is some overlap with one sample from location 2 (Figure 2). The basalts from location 1, which are lavas erupted onto the surface, may have undergone a larger degree of degassing relative to the intruded dolerites (which were emplaced at depths

of  $>1$  km), which may explain some of the observed depletion in chlorine. Chlorine partitions into a hydrous magmatic vapor during decompression, which may then be outgassed (Webster et al., 1999). The magnitude of chlorine degassing, however, is difficult to estimate from these data. The proportion of Cl degassing from basalt lava flows is estimated to lie in the

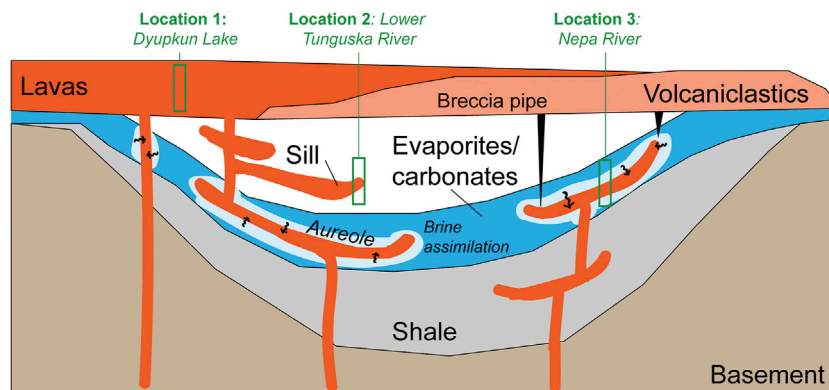


**FIGURE 7 |** Schematic diagram to show the general geological setting of the Siberian traps along an approximate N-S cross-section through the map in **Figure 1**, showing the contextual setting of each sampling area. Adapted from (Stordal et al., 2017). Location 1 samples (Dyupkun Lake) are basalt lavas erupted onto basin sediments. Location 2 samples (Lower Tunguska River) are dolerites from sills intruded into terrigenous sediments. Location 3 samples (Nepa River) are dolerite from sills intruded into evaporites, sampled from a borehole. The schematic reflects our conclusions that although the dolerites from location 3 show the strongest halogen enrichment signatures arising from brine assimilation from the evaporite contact aureoles, all magmas in the Siberian Traps Province likely have some interaction with both terrigenous sediments and evaporites at depth in the basin sequence.

range 27–72% for other flood basalt eruptions (Thordarson and Self, 1993; Thordarson et al., 1996; Self et al., 2008) consistent with experimental studies on basalts and andesites which have yielded aqueous fluid-silicate melt partition coefficients for Cl of between 1 and ~20 (Bureau et al., 1998; Webster et al., 1999; Villemant et al., 2008).

## Thermal and Geochemical Modeling of Sill Emplacement

Magmas intruded into volatile-rich sediments, such as evaporites, can cause extensive outgassing well as partial melting of the sediment (Aarnes et al., 2011a; Iacono-Marziano et al., 2012). To understand how the evaporites are affected by sill intrusions, a one-dimensional thermal model for sill emplacement into country rocks is developed, incorporating the thermal properties of pure halite (NaCl) and the thermal convection of

magma (details of the model and the code may be found in the **Supplementary Material**). We note that most evaporites contain additional chemical components, which will affect the solidus temperature, as well as H<sub>2</sub>O (Grishina et al., 2018). We choose a host rock starting temperature of 50°C, but acknowledge that the host rocks may have been hotter, which would affect the results. The thermal modeling results using the parameters listed in **Supplementary Material** for thick (40 m) and thin (2 m) intrusions are shown in **Figures 6A,B**. Br and Cl loss was modeled based on the heating experiments carried out by Svensen et al. (2009) that show Br and Cl halocarbon formation in evaporites heated to 275°C. In reality, devolatilization might begin at lower temperatures, although very little published data exist for evaporite's phase stability. Importantly, convection in magma has the consequence that heat transfer occurs faster. Thus, a 40 m thick sill emplaced at 1,200°C produces melting of a 7 m thick layer on the upper contact. In

**TABLE 3 |** Estimates of the proportion of chlorine (Cl) assimilated by the magmas that formed the whole rocks analysed in this study, using the method of Kendrick et al. (2013 (described in main text). Sample Br/Cl and Cl contents (ppm) are shown (also shown in **Table 1**). Assimilated Cl (%) is estimated based on a mass balance, using values of Br/Cl of  $2.8 \pm 0.8 \times 10^{-3}$  for the mantle and  $0.3 \times 10^{-3}$  for brines derived from evaporites (Kendrick et al., 2017).

Location	Br/Cl	Cl, ppm	Assimilated Cl, %	Primary Cl, ppm
1: Dyupkun Lake	4.3	92	—	92
	6.6	151	—	151
	7.9	63	—	63
2: Lower Tunguska River	4.3	325	—	325
	0.24	5331	—	—
	0.64	1569	82–89	172–281
	0.68	2068	80–88	253–414
3: Nepa River borehole	1.3	3022	47–68	975–1591
	2.2	1852	0–39	1135–1852
	1.1	4143	58–74	1069–1744
	1.2	2307	53–71	670–1093
	1.6	3675	32–58	1541–2514

contrast, the aureole affected by Cl and Br devolatilization is 29 m thick on the upper contact and 23.5 m on the lower contact (**Figure 6A**). If the magma temperature is initially 1,100°C (i.e., 100° lower), the molten salt layer on the top of the sill is 1.5 m thick (**Figure 6C**), and for a temperature of 1,090°C, no melting of the salt strata occurs (**Figure 6D**). There is no melting for a thin intrusion (2 m) even when the surrounding salt reaches the highest temperature of 1,200°C, and the thickness affected by devolatilization is 4.24 on the top margin and 4.09 m on the bottom margin of the intrusion (**Figure 6B**). These models are consistent with previous estimates reporting the aureole thickness to be typically within 30–250% of the intrusion's thickness (Aarnes et al., 2010). Moreover, it has been suggested that hydrocarbon generation by devolatilization may increase by nearly 35% in the case of two separate sills emplaced in organic-rich sediments with a vertical spacing of 5–10 times the intrusion thickness (Aarnes et al., 2011a), over the sum of the effects of two entirely separate sills.

Thermal modeling demonstrates that if the basalt temperature is < 1,100°C, melting of the evaporites is negligible. Therefore, congruent melting and assimilation of melted evaporite is not the mechanism leading to halogen enrichment in the intruded magma. Further, if the sill had assimilated evaporites by congruent melting, the sills would be enriched in all halogen species that are found in the evaporites (Cl, Br, and I), as well as Na and K, which is not observed (see whole rock compositions plotted in **Supplementary Material Figure S2 and S3**). Instead, we suggest that the geochemical trends are consistent with halogens being assimilated into the magma in the form of brine. Thermal models suggest that the metamorphic aureole within which devolatilization of halogens is possible may extend to several tens of meters for the case of discrete emplacement of a 40-m thick sill. In reality, the aureole's devolatilized region will be larger than modeled as the evaporite is likely to contain salts with lower melting and devolatilization temperatures (i.e., sylvite, carnallite) (Grishina et al., 1992). Water is driven off the heated sediments, and halogens (and other elements) will partition into the hydrothermal fluids produced. The increasing Br content of the evaporites with decreasing distance from the dolerite contact, particularly at the lower contact (**Figure 4; Table 2**) may reflect the accumulation of heating-derived fluids in pore spaces in the salt, with the evaporites beneath the dolerite trapping more fluid as a consequence of the low permeability of the overlying dolerite, a pattern also observed in previous studies of total organic carbon content of shales intruded by dolerite sills (Aarnes et al., 2011b). At low pressures and high temperatures, the hydrothermal fluids produced during heating of evaporites will comprise a coexisting brine and vapor (Liebscher et al., 2006; Coumou et al., 2009; Kendrick and Burnard, 2013). It is not well understood whether fractionation of Br and Cl occurs during the phase separation stage (Kendrick, 2018). Data from conjugate vapor and brine fluids from hydrothermal vents, for example, have similar Br/Cl ratios (Von Damm et al., 1997; Wu et al., 2012) which is consistent with experimental data (Berndt and Seyfried, 1997). We propose that the separated, low-density vapor phase migrated up towards the

surface, perhaps through permeable country rocks or explosively through gas pipes, as was described and demonstrated experimentally by Svensen et al. (2009). A circulating hydrothermal system may have allowed the higher density brine to follow activity gradients to become assimilated into the sill, as was demonstrated for intrusions in Duluth, Minnesota, where the flow of hydrothermal brines into sills has been identified based on osmium isotopic variations (Ripley et al., 2001). Sill solidification may also be accompanied by the formation of pressure gradients from the aureole into the sill (Galerne et al., 2010; Svensen et al., 2010; Iyer et al., 2018). The brine's ability to flow into the sill is supported by observations of veins and fissures in the sill filled in with salt precipitates 5–8 m from the contacts. In addition, high chlorine concentration on the rims of biotites in sills in the Lower Tunguska area have been interpreted as being due to chlorine transfer via a hydrous fluid (Heimdal et al., 2019; Callegaro et al., 2021) as observed for aureoles surrounding mafic sills at Norilsk (Pang et al., 2013).

The thermal modelling, combined with the geochemical data, suggests that many, if not all, samples in the set analysed here have been affected by assimilation of brines derived from heating evaporites in the subsurface prior to or during emplacement. Given these findings, we may use the geochemical data shown in **Figure 3D** to estimate the proportion of the Cl in the samples that was assimilated from a brine derived from heating evaporites. We use the method developed for estimating the amount of brine assimilation undergone by submarine magmas (Kendrick et al., 2013) whereby:

$$\%Cl_{\text{assimilated}} = 100 \times \left( 1 - \left( \frac{\left( \frac{Br}{Cl} \right)_{WR} - \left( \frac{Br}{Cl} \right)_{\text{brine}}}{\left( \frac{Br}{Cl} \right)_{\text{mantle}} - \left( \frac{Br}{Cl} \right)_{\text{brine}}} \right) \right)$$

The results of the analysis are shown in **Table 3**. The basalts from location 1 (Dyupkun Lake) may have been affected by degassing, so we do not discuss these further. The dolerites from the Lower Tunguska River (location 2) and the Nepa River borehole (location 3), likely assimilated between 0 and 89% of their chlorine contents during interaction with evaporite-derived brines. These upper values are similar to those estimated for the most contaminated submarine glasses from the Galápagos Spreading Centre and Lau Basin (~95%) (Kendrick et al., 2013). Using the observed Cl concentrations (**Table 1**), we may therefore estimate the “primary” Cl contents of the melts that formed these rocks (prior to Cl assimilation), which likely ranged from 172 to 2,514 ppm (**Table 3**).

## CONCLUSION

We present whole-rock trace and halogen concentrations for a suite of samples from three locations in the Siberian Traps Large Igneous Province. The samples comprise basalt lava flows from Dyupkun Lake, dolerite sills from the Lower Tunguska River (intruded into organic-rich shales), and a dolerite sill intruded into evaporites from a borehole in the Nepa River region. The data show that the dolerites are enriched in Cl, similar to MORB

and OIB that have been inferred to have assimilated seawater, and show halogen systematics which extend towards both evaporites and crustal brines. Furthermore, all analyzed samples show enrichment in Rb/Nb; with the dolerites also showing enrichment in Cl/K similar to MORB and OIB that have been inferred to have assimilated seawater. We interpret the data to show that samples from all three locations have assimilated components of crustal sediments (which include evaporites) (Figure 7). We estimate that dolerites in our sample set have assimilated up to 89% of their Cl from fluids derived from evaporites. Primary Cl contents of the magmas that formed the whole rocks analysed here (prior to contamination) may have ranged from 172 to 2,514 ppm. Halogen assimilation from subcropping evaporites may be pervasive throughout the region, regardless of whether or not the magmas are emplaced within evaporites (Figure 7). The basaltic lava flows from Dyupkun Lake have undergone degassing at atmospheric pressure, which has depleted their Cl contents.

Thermal modeling shows that the intrusion of a sill of a few tens of meters thickness, active over timescales of a few years, causes the evaporites surrounding the sill to become depleted in halogens through devolatilization, whereby heating drives off water and halogens partition into a hot aqueous fluid. At low pressures in the crust, where we envisage much of the sill emplacement to have occurred, phase separation into a low-density vapor and a higher density brine would occur. Basaltic magmas in the sill may assimilate such brines, becoming enriched in halogens. Vapor-transported halogens may have been outgassed to the atmosphere (via pipes or a permeable fracture network). These mechanisms of magmatic halogen assimilation from evaporites have implications for the amounts of Br and Cl reaching the atmosphere during both intrusive (whereby magmatism is dominated by sill emplacement) and extrusive activity (dominated by surface lavas flows).

## REFERENCES

- Aarnes, I., Fristad, K., Planke, S., and Svensen, H. (2011a). The Impact of Host-rock Composition on Devolatilization of Sedimentary Rocks during Contact Metamorphism Around Mafic Sheet Intrusions. *Geochem. Geophys. Geosystems* 12 (10). doi:10.1029/2011gc003636
- Aarnes, I., Svensen, H., Connolly, J. A. D., and Podladchikov, Y. Y. (2010). How Contact Metamorphism Can Trigger Global Climate Changes: Modeling Gas Generation Around Igneous Sills in Sedimentary Basins. *Geochimica et Cosmochimica Acta* 74 (24), 7179–7195. doi:10.1016/j.gca.2010.09.011
- Aarnes, I., Svensen, H., Polteau, S., and Planke, S. J. C. G. (2011b). Contact Metamorphic Devolatilization of Shales in the Karoo Basin, South Africa, and the Effects of Multiple Sill Intrusions. 281(3–4), 181–194. doi:10.1016/j.chemgeo.2010.12.007
- Asafov, E. V., Sobolev, A. V., Batanova, V. G., and Portnyagin, M. V. (2020). Chlorine in the Earth's Mantle as an Indicator of the Global Recycling of Oceanic Crust. *Russ. Geology. Geophys.* 61 (9), 937–950. doi:10.15372/rgg2020161
- Beerling, D. J., Harfoot, M., Lomax, B., and Pyle, J. A. (2007). The Stability of the Stratospheric Ozone Layer during the End-Permian Eruption of the Siberian Traps. *Phil. Trans. R. Soc. A*. 365 (1856), 1843–1866. doi:10.1098/rsta.2007.2046
- Benca, J. P., Duijnste, I. A. P., and Looy, C. V. (2018). UV-B-induced forest Sterility: Implications of Ozone Shield Failure in Earth's Largest Extinction. *Sci. Adv.* 4 (2), e1700618. doi:10.1126/sciadv.1700618

## DATA AVAILABILITY STATEMENT

The original contributions presented in the study are included in the article/**Supplementary Material**, further inquiries can be directed to the corresponding author.

## AUTHOR CONTRIBUTIONS

SS analysed the samples. All authors interpreted the data and co-wrote the manuscript.

## ACKNOWLEDGMENTS

We thank Taras Gerya (ETH-Zurich, Switzerland) and Jerome Neufeld (BP Institute, United Kingdom) for their advice on thermal modeling. We acknowledge the Geological Society of London for research grant funding; and Natural Environment Research Council grant NE/H012648/1. SS acknowledges Trinity Hall College (Cambridge, United Kingdom) for providing a Mann Studentship to fund her Ph.D. studies. AGP was partially funded by RFBR grants (18-05-00682 and 18-05-70073). The Norwegian Research Council is acknowledged for supporting HS and SP through a Centre of Excellence grant to CEED (project number 223272).

## SUPPLEMENTARY MATERIAL

The Supplementary Material for this article can be found online at: <https://www.frontiersin.org/articles/10.3389/feart.2021.741447/full#supplementary-material>.

- Berndt, M. E., and Seyfried, W. E., Jr (1997). Calibration of Fractionation during Subcritical Phase Separation of Seawater: Possible Halite at 9 to 10<sup>6</sup>N East Pacific Rise. *Geochimica et Cosmochimica Acta* 61 (14), 2849–2854. doi:10.1016/s0016-7037(97)00134-8
- Black, B. A., Elkins-Tanton, L. T., Rowe, M. C., and Peate, I. U. (2012). Magnitude and Consequences of Volatile Release from the Siberian Traps. *Earth Planet. Sci. Lett.* 317–318, 363–373. doi:10.1016/j.epsl.2011.12.001
- Black, B. A., Lamarque, J.-F., Shields, C. A., Elkins-Tanton, L. T., and Kiehl, J. T. (2014). Acid Rain and Ozone Depletion from Pulsed Siberian Traps Magmatism. 42(1), 67–70. doi:10.1130/g34875.1
- Black, B. A., Neely, R. R., Lamarque, J.-F., Elkins-Tanton, L. T., Kiehl, J. T., Shields, C. A., et al. (2018). Systemic Swings in End-Permian Climate from Siberian Traps Carbon and Sulfur Outgassing. *Nat. Geosci* 11 (12), 949–954. doi:10.1038/s41561-018-0261-y
- Bobrowski, N., Hönninger, G., Galle, B., and Platt, U. (2003). Detection of Bromine Monoxide in a Volcanic Plume. *Nature* 423 (6937), 273–276. doi:10.1038/nature01625
- Broadley, M. W., Barry, P. H., Ballentine, C. J., Taylor, L. A., and Burgess, R. (2018). End-Permian Extinction Amplified by Plume-Induced Release of Recycled Lithospheric Volatiles. *Nat. Geosci* 11 (9), 682–687. doi:10.1038/s41561-018-0215-4
- Bureau, H., Pineau, F., Métrich, N., Semet, M., and Javoy, M. (1998). A melt and fluid inclusion study of the gas phase at Piton de la Fournaise volcano (Réunion Island). *Chem. Geology*. 147 (1), 115–130. doi:10.1016/s0009-2541(97)00176-9

- Burgess, S. D., Bowring, S., and Shen, S.-z. (2014). High-precision Timeline for Earth's Most Severe Extinction. *Proc. Natl. Acad. Sci. USA* 111 (9), 3316–3321. doi:10.1073/pnas.1317692111
- Burgess, S. D., Muirhead, J. D., and Bowring, S. A. (2017). Initial Pulse of Siberian Traps Sills as the Trigger of the End-Permian Mass Extinction. *Nat. Commun.* 8 (1), 164. doi:10.1038/s41467-017-00083-9
- Callegaro, S., Svensen, H., Neumann, E., Polozov, A., Jerram, D., Deegan, F., et al. (2021). Geochemistry of Deep Tunguska Basin Sills, Siberian Traps: Correlations and Potential Implications for the End-Permian Environmental Crisis. *176*(7), 1–30. doi:10.1007/s00410-021-01807-3
- Campbell, I. H., Czamanske, G. K., Fedorenko, V. A., Hill, R. L., and Stepanov, V. (1992). Synchronism of the Siberian Traps and the Permian-Triassic Boundary. *Science* 258 (5089), 1760–1763. doi:10.1126/science.258.5089.1760
- Coumou, D., Driesner, T., Weis, P., and Heinrich, C. A. (2009). Phase Separation, Brine Formation, and Salinity Variation at Black Smoker Hydrothermal Systems. *J. Geophys. Res. Solid Earth* 114 (B3). doi:10.1029/2008jb005764
- Czamanske, G. K., Wooden, J. L., Walker, R. J., Fedorenko, V. A., Simonov, O. N., Budahn, J. R., et al. (2000). Geochemical, Isotopic, and SHRIMP Age Data for Precambrian Basement Rocks, Permian Volcanic Rocks, and Sedimentary Host Rocks to the Ore-Bearing Intrusions, Noril'sk-Talnakh District, Siberian Russia. *Int. Geology. Rev.* 42 (10), 895–927. doi:10.1080/00206810009465117
- Daniel, J. S., Solomon, S., Portmann, R. W., and Garcia, R. R. (1999). Stratospheric Ozone Destruction: The Importance of Bromine Relative to Chlorine. *J. Geophys. Res.* 104 (D19), 23871–23880. doi:10.1029/1999jd900381
- Fedorenko, V., and Czamanske, G. (1997). Results of New Field and Geochemical Studies of the Volcanic and Intrusive Rocks of the Maymecha-Kotuy Area, Siberian Flood-basalt Province, Russia. *Int. Geology. Rev.* 39 (6), 479–531. doi:10.1080/00206819709465286
- Galerne, C. Y., Neumann, E.-R., Aarnes, I., and Planke, S. (2010). Magmatic Differentiation Processes in Saucer-Shaped Sills: Evidence from the Golden Valley Sill in the Karoo Basin, South Africa. *South Africa* 6 (3), 163–188. doi:10.1130/ges00500.1
- Gerlach, T. (2004). Volcanic Sources of Tropospheric Ozone-depleting Trace Gases. *Geochem. Geophys. Geosystems* 5 (9). doi:10.1029/2004gc000747
- Grishina, S., Dubessy, J., Kontorovich, A., and Pironon, J. (1992). Inclusions in Salt Beds Resulting from thermal Metamorphism by Dolerite Sills (Eastern Siberia, Russia). *ejm* 4, 1187–1202. doi:10.1127/ejm/4/5/1187
- Grishina, S., Dubessy, J., Kontorovich, A., and Pironon, J. J. P. (1991). Metamorphic Fluids of Evaporite: A Case Study Exemplified by Fluid Inclusions from Cambrian Salt Deposits and Oil and Gas Zones Intruded by Dolerite Sills (Siberia, USSR). (5), 94–95.
- Grishina, S., Koděra, P., Goryainov, S., Oreshonkov, A., Seryotkin, Y., Šimko, F., et al. (2020). Application of Raman Spectroscopy for Identification of Rinneite (K<sub>3</sub>NaFeCl<sub>6</sub>) in Inclusions in Minerals. *J. Raman Spectrosc.* 51 (12), 2505–2516. doi:10.1002/jrs.6005
- Grishina, S., Koděra, P., Uriarte, L. M., Dubessy, J., Oreshonkov, A., Goryainov, S., et al. (2018). Identification of Anhydrous CaCl<sub>2</sub> and KCaCl<sub>3</sub> in Natural Inclusions by Raman Spectroscopy. *Chem. Geology.* 493, 532–543. doi:10.1016/j.chemgeo.2018.07.017
- Hawkesworth, C., Lightfoot, P., Fedorenko, V., Blake, S., Naldrett, A., Doherty, W., et al. (1995). Magma Differentiation and Mineralisation in the Siberian continental Flood Basalts. *34*(1-3), 61–88. doi:10.1016/0024-4937(95)90011-x
- Heimdal, T. H., Callegaro, S., Svensen, H. H., Jones, M. T., Pereira, E., and Planke, S. (2019). Evidence for Magma-Evaporite Interactions during the Emplacement of the Central Atlantic Magmatic Province (CAMP) in Brazil. *Earth Planet. Sci. Lett.* 506, 476–492. doi:10.1016/j.epsl.2018.11.018
- Iacono-Marziano, G., Marecal, V., Pirre, M., Gaillard, F., Arteta, J., Scaillet, B., et al. (2012). Gas Emissions Due to Magma-Sediment Interactions during Flood Magmatism at the Siberian Traps: Gas Dispersion and Environmental Consequences. *Earth Planet. Sci. Lett.* 357-358, 308–318. doi:10.1016/j.epsl.2012.09.051
- Istomin, V., Mazurov, M., and Grishina, S. (2000). Typomorphism of Paramagnetic Impurities in Halites from the Zones of Basic-Rock-Evaporite Interaction (Siberian Platform). *Geologiya i Geofizika*, 41, 126–134.
- Iyer, K., Svensen, H., and Schmid, D. W. (2018). SILLi 1.0: a 1-D Numerical Tool Quantifying the thermal Effects of Sill Intrusions. *Geosci. Model. Dev.* 11 (1), 43–60. doi:10.5194/gmd-11-43-2018
- Jarvis, I., and Jarvis, K. E. (1992). Plasma Spectrometry in the Earth Sciences: Techniques, Applications and Future Trends. *Chem. Geology.* 95 (1-2), 1–33. doi:10.1016/0009-2541(92)90041-3
- Kendrick, M. A., Arculus, R., Burnard, P., and Honda, M. (2013). Quantifying Brine Assimilation by Submarine Magmas: Examples from the Galápagos Spreading Centre and Lau Basin. *Geochimica et Cosmochimica Acta* 123, 150–165. doi:10.1016/j.gca.2013.09.012
- Kendrick, M. A., and Burnard, P. (2013). *The noble Gases as Geochemical Tracers*. Springer, 319–369. doi:10.1007/978-3-642-28836-4\_11 Noble Gases and Halogens in Fluid Inclusions: A Journey through the Earth's Crust
- Kendrick, M. A., Caulfield, J. T., Nguyen, A. D., Zhao, J.-x., and Blakey, I. (2020). Halogen and Trace Element Analysis of Carbonate-Veins and Fe-Oxyhydroxide by LA-ICPMS: Implications for Seafloor Alteration, Atlantis Bank, SW Indian Ridge. *Chem. Geology.* 547, 119668. doi:10.1016/j.chemgeo.2020.119668
- Kendrick, M. A. (2018). "Halogens in Seawater, marine Sediments and the Altered Oceanic Lithosphere," in *The Role of Halogens in Terrestrial and Extraterrestrial Geochemical Processes* (Springer), 591–648. doi:10.1007/978-3-319-61667-4\_9
- Kendrick, M. A., Hémond, C., Kamenetsky, V. S., Danyushevsky, L., Devey, C. W., Rodemann, T., et al. (2017). Seawater Cycled throughout Earth's Mantle in Partially Serpentinized Lithosphere. *Nat. Geosci* 10 (3), 222–228. doi:10.1038/Ngeo2902
- Kendrick, M. A., Kamenetsky, V. S., Phillips, D., and Honda, M. (2012). Halogen Systematics (Cl, Br, I) in Mid-ocean ridge Basalts: a Macquarie Island Case Study. *Geochimica et Cosmochimica Acta* 81, 82–93. doi:10.1016/j.gca.2011.12.004
- Le Vaillant, M., Barnes, S. J., Mungall, J. E., and Mungall, E. L. (2017). Role of Degassing of the Noril'sk Nickel Deposits in the Permian-Triassic Mass Extinction Event. *Proc. Natl. Acad. Sci.* 114, 2485–2490. doi:10.1073/pnas.1611086114
- Liebscher, A., Barnes, J., and Sharp, Z. (2006). Chlorine Isotope Vapor-Liquid Fractionation during Experimental Fluid-phase Separation at 400 C/23 MPa to 450 C/42 MPa. *Chem. Geology.* 234 (3-4), 340–345. doi:10.1016/j.chemgeo.2006.04.009
- Lightfoot, P. C., Naldrett, A. J., Gorbachev, N. S., Doherty, W., and Fedorenko, V. A. (1990). Geochemistry of the Siberian Trap of the Noril'sk Area, USSR, with Implications for the Relative Contributions of Crust and Mantle to Flood basalt Magmatism. *Contr. Mineral. Petrol.* 104 (6), 631–644. doi:10.1007/bf011167284
- Lomax, B., Beerling, D., Callaghan, T., Fraser, W., Harfoot, M., Pyle, J., et al. (2005). *The Siberian Traps, Stratospheric Ozone, UV-B Flux, and Mutagenesis. Earth Systems Processes 2, Calgary 8–11 August 2005 Paper 37-3*. Available at: [http://gsa.confex.com/gsa/2005ESP/finalprogram/abstract\\_88582.htm](http://gsa.confex.com/gsa/2005ESP/finalprogram/abstract_88582.htm).
- Malich, N., Tazihin, N., Tuganova, E., Bunzen, E., Kulikova, N., and Safonova, I. (1974). *Map of Geological Formations of the Siberian Platform Cover (1: 500 000)*. Leningrad: All-Union Research Geologic Institute (VSEGEI).
- Mazurov, M. P., Grishina, S. N., Istomin, V. E., and Titov, A. T. (2007). Metasomatism and Ore Formation at Contacts of Dolerite with Saliferous Rocks in the Sedimentary Cover of the Southern Siberian Platform. *Geol. Ore Deposits* 49 (4), 271–284. doi:10.1134/s1075701507040022
- McCaffrey, M. A., Lazar, B., and Holland, H. D. (1987). The Evaporation Path of Seawater and the Coprecipitation of Br- and K+ with Halite. *J. Sediment. Petrol.* 57 (5), 928–938. doi:10.1306/212f8cab-2b24-11d7-8648000102c1865d
- McDonough, W. F., and Sun, S. s. (1995). The Composition of the Earth. *Chem. Geology.* 120(3-4), 223–253. doi:10.1016/0009-2541(94)00140-4
- Michael, P. J., and Cornell, W. C. (1998). Influence of Spreading Rate and Magma Supply on Crystallization and Assimilation beneath Mid-ocean Ridges: Evidence from Chlorine and Major Element Chemistry of Mid-ocean ridge Basalts. *J. Geophys. Res.* 103 (B8), 18325–18356. doi:10.1029/98jb00791
- Michel, A., and Villemant, B. (2003). Determination of Halogens (F, Cl, Br, I), Sulfur and Water in Seventeen Geological Reference Materials. *Geostandards Newsl.* 27 (2), 163–171. doi:10.1111/j.1751-908x.2003.tb00643.x
- Neumann, E.-R., Svensen, H. H., Polozov, A. G., and Hammer, Ø. (2017). Formation of Si-Al-Mg-Ca-Rich Zoned Magnetite in an End-Permian Phreatomagmatic Pipe in the Tunguska Basin, East Siberia. *Miner Deposita* 52 (8), 1205–1222. doi:10.1007/s00126-017-0717-9

- Oppenheimer, C., Tsanev, V. I., Braban, C. F., Cox, R. A., Adams, J. W., Aiuppa, A., et al. (2006). BrO Formation in Volcanic Plumes. *Geochimica et Cosmochimica Acta* 70 (12), 2935–2941. doi:10.1016/j.gca.2006.04.001
- Pang, K.-N., Arndt, N., Svensen, H., Planke, S., Polozov, A., Polteau, S., et al. (2013). A Petrologic, Geochemical and Sr-Nd Isotopic Study on Contact Metamorphism and Degassing of Devonian Evaporites in the Noril'sk Aureoles, Siberia. *Contrib. Mineral. Petrol.* 165 (4), 683–704. doi:10.1007/s00410-012-0830-9
- Payne, J. L., Lehrmann, D. J., Wei, J., Orchard, M. J., Schrag, D. P., and Knoll, A. H. (2004). Large Perturbations of the Carbon Cycle during Recovery from the End-Permian Extinction. *Science* 305 (5683), 506–509. doi:10.1126/science.1097023
- Petrychenko, Y., Peryt, T. M., and Chechel, E. I. (2005). Early Cambrian Seawater Chemistry from Fluid Inclusions in Halite from Siberian Evaporites. *Chem. Geology*. 219 (1-4), 149–161. doi:10.1016/j.chemgeo.2005.02.003
- Polozov, A. G., Svensen, H. H., Planke, S., Grishina, S. N., Fristad, K. E., and Jerram, D. A. (2016). The basalt Pipes of the Tunguska Basin (Siberia, Russia): High Temperature Processes and Volatile Degassing into the End-Permian Atmosphere. *Palaeogeogr. Palaeoclimatol. Palaeoecol.* 441, 51–64. doi:10.1016/j.palaeo.2015.06.035
- Rampino, M. R., Rodriguez, S., Baransky, E., and Cai, Y. (2017). Global Nickel Anomaly Links Siberian Traps Eruptions and the Latest Permian Mass Extinction. *Sci. Rep.* 7 (1), 12416–6. doi:10.1038/s41598-017-12759-9
- Reichow, M. K., Pringle, M., Al'Mukhamedov, A., Allen, M., Andreichev, V., Buslov, M., et al. (2009). The Timing and Extent of the Eruption of the Siberian Traps Large Igneous Province: Implications for the End-Permian Environmental Crisis. *Earth Planet. Sci. Lett.* 277 (1), 9–20. doi:10.1016/j.epsl.2008.09.030
- Reichow, M. K., Saunders, A., White, R., Al'Mukhamedov, A., and Medvedev, A. Y. (2005). Geochemistry and Petrogenesis of Basalts from the West Siberian Basin: an Extension of the Permo-Triassic Siberian Traps, Russia. *Lithos* 79 (3-4), 425–452. doi:10.1016/j.lithos.2004.09.011
- Renne, P. R., and Basu, A. R. (1991). Rapid Eruption of the Siberian Traps Flood Basalts at the Permo-Triassic Boundary. *Science* 253 (5016), 176–179. doi:10.1126/science.253.5016.176
- Renne, P. R., Black, M. T., Zichao, Z., Richards, M. A., and Basu, A. R. (1995). Synchrony and Causal Relations between Permian-Triassic Boundary Crises and Siberian Flood Volcanism. *Science* 269 (5229), 1413–1416. doi:10.1126/science.269.5229.1413
- Ripley, E. M., Park, Y.-R., Lambert, D. D., and Frick, L. R. (2001). Re-Os Isotopic Variations in Carbonaceous Pelites Hosting the Duluth Complex: Implications for Metamorphic and Metasomatic Processes Associated with Mafic Magma chambers. *Geochimica et Cosmochimica Acta* 65 (17), 2965–2978. doi:10.1016/s0016-7037(01)00635-4
- Rothman, D. H., Fournier, G. P., French, K. L., Alm, E. J., Boyle, E. A., Cao, C., et al. (2014). Methanogenic Burst in the End-Permian Carbon Cycle. *Proc. Natl. Acad. Sci.* 111 (15), 5462–5467. doi:10.1073/pnas.1318106111
- Self, S., Blake, S., Sharma, K., Widdowson, M., and Sephton, S. (2008). Sulfur and Chlorine in Late Cretaceous Deccan Magmas and Eruptive Gas Release. *Science* 319 (5870), 1654–1657. doi:10.1126/science.1152830
- Self, S., Thordarson, T., and Widdowson, M. (2005). Gas Fluxes from Flood basalt Eruptions. *Elements* 1(5), 283–287. doi:10.2113/gselements.1.5.283
- Shen, S.-Z., Ramezani, J., Chen, J., Cao, C.-Q., Erwin, D. H., Zhang, H., et al. (2019). A Sudden End-Permian Mass Extinction in South China. *131*(1-2), 205–223. doi:10.1130/b31909.1
- Sibik, S., Edmonds, M., MacLennan, J., and Svensen, H. (2015). Magmas Erupted during the Main Pulse of Siberian Traps Volcanism Were Volatile-Poor. *J. Petrology* 56 (11), 2089–2116. doi:10.1093/petrology/egv064
- Sinnhuber, B.-M., Sheode, N., Sinnhuber, M., Chipperfield, M. P., and Feng, W. (2009). The Contribution of Anthropogenic Bromine Emissions to Past Stratospheric Ozone Trends: a Modelling Study. *Atmos. Chem. Phys.* 9 (8), 2863–2871. doi:10.5194/acp-9-2863-2009
- Sobolev, A. V., Krivolutsкая, N. A., and Kuzmin, D. V. (2009). Petrology of the Parental Melts and Mantle Sources of Siberian Trap Magmatism. *Petrology* 17 (3), 253–286. doi:10.1134/s0869591109030047
- Sobolev, S. V., Sobolev, A. V., Kuzmin, D. V., Krivolutsкая, N. A., Petrunin, A. G., Arndt, N. T., et al. (2011). Linking Mantle Plumes, Large Igneous Provinces and Environmental Catastrophes. *Nature* 477 (7364), 312–316. doi:10.1038/nature10385
- Stordal, F., Svensen, H. H., Aarnes, I., Roscher, M., and Palaeoclimatology, Palaeoecology. (2017). Global Temperature Response to century-scale Degassing from the Siberian Traps Large Igneous Province. *Palaeogeogr. Palaeoclimatol. Palaeoecol.* 471, 96–107. doi:10.1016/j.palaeo.2017.01.045
- Svensen, H., Aarnes, I., Podladchikov, Y. Y., Jettestuen, E., Harstad, C. H., and Planke, S. (2010). Sandstone Dikes in Dolerite Sills: Evidence for High-Pressure Gradients and Sediment Mobilization during Solidification of Magmatic Sheet Intrusions in Sedimentary Basins. *6*(3), 211–224. doi:10.1130/ges00506.1
- Svensen, H. H., Frolov, S., Akhmanov, G. G., Polozov, A. G., Jerram, D. A., Shiganova, O. V., et al. (2018). Sills and Gas Generation in the Siberian Traps. *Phil. Trans. R. Soc. A.* 376 (2130), 20170080. doi:10.1098/rsta.2017.0080
- Svensen, H., Planke, S., Polozov, A. G., Schmidbauer, N., Corfu, F., Podladchikov, Y. Y., et al. (2009). Siberian Gas Venting and the End-Permian Environmental Crisis. *Earth Planet. Sci. Lett.* 277 (3), 490–500. doi:10.1016/j.epsl.2008.11.015
- Thordarson, T., Self, S., Oskarsson, N., and Hulsebosch, T. (1996). Sulfur, Chlorine, and Fluorine Degassing and Atmospheric Loading by the 1783–1784 AD Laki (Skaftár Fires) Eruption in Iceland. *Bull. Volcanology* 58 (2-3), 205–225. doi:10.1007/s004450050136
- Thordarson, T., and Self, S. (1993). The Laki (Skaftár Fires) and Grímsvötn Eruptions in 1783/1785. *Bull. Volcanol* 55 (4), 233–263. doi:10.1007/BF00624353
- Vasil'ev, Y. R., Zolotukhin, V., Feoktistov, G., and Prusskaya, S. J. Г. и. Г. (2000). Evaluation of the Volumes and Genesis of Permo-Triassic Trap Magmatism on the Siberian Platform. *41*(12), 1696–1705.
- Villemant, B., Mouatt, J., and Michel, A. (2008). Andesitic Magma Degassing Investigated through H<sub>2</sub>O Vapour-Melt Partitioning of Halogens at Soufrière Hills Volcano, Montserrat (Lesser Antilles). *Earth Planet. Sci. Lett.* 269 (1-2), 212–229. doi:10.1016/j.epsl.2008.02.014
- Von Damm, K. L., Buttermore, L., Oosting, S., Bray, A., Fornari, D., Lilley, M., et al. (1997). Direct Observation of the Evolution of a Seafloor 'black Smoker' from Vapor to Brine. *149*(1-4), 101–111. doi:10.1016/s0012-821x(97)00059-9
- Webster, J. D., Kinzler, R. J., and Mathez, E. A. (1999). Chlorine and Water Solubility in basalt and Andesite Melts and Implications for Magmatic Degassing. *Geochimica et Cosmochimica Acta* 63 (5), 729–738. doi:10.1016/s0016-7037(99)00043-5
- Wooden, J. L., Czamanske, G. K., Fedorenko, V. A., Arndt, N. T., Chauvel, C., Bouse, R. M., et al. (1993). Isotopic and Trace-Element Constraints on Mantle and Crustal Contributions to Siberian continental Flood Basalts, Noril'sk Area, Siberia. *Geochimica et Cosmochimica Acta* 57 (15), 3677–3704. doi:10.1016/0016-7037(93)90149-q
- Wu, S.-F., You, C.-F., Valsami-Jones, E., Baltatzis, E., and Shen, M.-L. (2012). Br/Cl and I/Cl Systematics in the Shallow-Water Hydrothermal System at Milos Island, Hellenic Arc. *Mar. Chem.* 140-141, 33–43. doi:10.1016/j.marchem.2012.07.004
- Zharkov, M. A. (1984). *Paleozoic Salt Bearing Formations of the World*. Springer-Verlag.
- Zherebtsova, I., and Volkova, N. (1966). Experimental Study of Behavior of Trace Elements in the Process of Natural Solar Evaporation of Black Sea Water and Sasyk-Sivash Brine. *Geochem. Int.* 3 (4), 656–670.

**Conflict of Interest:** The authors declare that the research was conducted in the absence of any commercial or financial relationships that could be construed as a potential conflict of interest.

**Publisher's Note:** All claims expressed in this article are solely those of the authors and do not necessarily represent those of their affiliated organizations, or those of the publisher, the editors, and the reviewers. Any product that may be evaluated in this article, or claim that may be made by its manufacturer, is not guaranteed or endorsed by the publisher.

Copyright © 2021 Sibik, Edmonds, Villemant, Svensen, Polozov and Planke. This is an open-access article distributed under the terms of the Creative Commons Attribution License (CC BY). The use, distribution or reproduction in other forums is permitted, provided the original author(s) and the copyright owner(s) are credited and that the original publication in this journal is cited, in accordance with accepted academic practice. No use, distribution or reproduction is permitted which does not comply with these terms.